JAERI-M
88-153

DEPENDENCE OF COUPLING RESISTANCE ON TOROIDAL WAVE NUMBER SPECTRUM DURING H-MODE DISCHARGE

August 1988

Mikio SAIGUSA, Haruyuki KIMURA, Tsuneyuki FUJII, Noriyuki KOBAYASHI
Shin'ichi MORIYAMA, Katsuto ANNOH, Yoshirou OGAWA
Shin'ichi SHINOZAKI, Masayuki TERAKADO and JT-60 Team

日本原子力研究所
Japan Atomic Energy Research Institute

JAERI-Mレポートは，日本原子力研究所が不定期に公刊している研究報告書です。
入手の問合わせは，日本原子力研究所技術情報部情報資料課（〒319-11茨城県那珂郡東海村）あて，お申しこしください。なお，このほかに財団法人原子力弘済会資料センター（〒319-11 茨城県那珂郡東海村日本原子力研究所内）で複写による実費頒布をおこなっております。

JAERI-M reports are issued irregularly.
Inquiries about availability of the reports should be addressed to Information Division Department of Technical Information, Japan Atomic Energy Research Institute, Tokai-mura, Naka-gun, Ibaraki-ken 319-11, Japan.

編集兼発行　日本原子力研究所
印　　刷　㈱高野高速印刷

Dependence of Coupling Resistance on Toroidal Wave Number Spectrum During H-mode Discharge

Mikio SAIGUSA, Haruyuki KIMURA[+], Tsuneyuki FUJII, Noriyuki KOBAYASHI
Shin'ichi MORIYAMA[++], Katsuto ANNOH[++], Yoshirou OGAWA[++]
Shin'ichi SHINOZAKI[++], Masayuki TERAKADO[++] and JT-60 Team

Department of Thermonulcear Fusion Research
Naka Fusion Research Establishment
Japan Atomic Energy Research Institute
Naka-machi, Naka-gun, Ibaraki-ken

(Received July 21, 1988)

The increase in coupling resistance of ICRF antenna during H-mode discharges is firstly investigated in JT-60. This interesting phenomena which were depended on $k_{\parallel}$ spectrum can be explained with the antenna-plasma coupling theory taking account of the antenna phasing and the electron density profiles. It became evident that the coupling resistance can be kept constant after H-mode transition by the optimum antenna design and the property control of antenna phasing. But the decrease in coupling resistance during H-mode discharge is predicted on the toroidal 4 loop antenna array designed for JT-60U ICRF launcher in high density regime.

Keywords; Coupling Resistance, ICRF Antenna, H-mode, Coupling Theory, JT-60, JT-60U

+ Fusion Experimental Reactor Team
++ Department of JT-60 Facility

Hモード遷移時におけるＩＣＲＦアンテナ負荷抵抗のトロイダル方向波数スペクトル依存性の研究

日本原子力研究所那珂研究所核融合研究部
三枝　幹雄・木村　晴行[+]・藤井　常幸・小林　則幸
森山　伸一[++]・安納　勝人[++]・小川　芳郎[++]・篠崎　信一[++]
寺門　正之[++]・ＪＴ－６０チーム

（１９８８年7月２１日受理）

ＪＴ－６０でHモード遷移時に他のトカマクでは減少するＩＣＲＦアンテナの負荷抵抗が増加する現象が初めて観測された。この現象は，アンテナアレイ間の位相差に依存しており，位相差とプラズマ密度分布を考慮したアンテナープラズマ結合理論により説明する事ができた。また，ＪＴ－６０Ｕのパラメータを用い，トロイダル方向に４列のアンテナアレイのHモード遷移時における結合特性を調べた結果，低密度領域では増加する結合抵抗も高密度領域では減少する事が理論的に予測された。

那珂研究所：〒311－01　茨城県那珂郡那珂町大字向山 801－1
＋　核融合実験炉特別チーム
++ ＪＴ－６０試験部

Contents

目　　次

1. INTRODUCTION

The investigation of the ICRF antenna coupling property during H-mode is very important for the improvement of the reliability on the ICRF heating system. A high voltage is generated in the transmission line and the output circuit of tetrode by mismatching after the H-transition, which decides often the upper limit of an injected power. Electron density profiles in the vicinity of the separatrix of a diverted discharge were measured in several tokamaks during the H-mode [1]. An electron density increases inside the separatrix surface and decreases in a scrape-off-layer (SOL) so that the density gradient on plasma edge becomes steeper after the H-transition. Unfavorable decrease in the coupling resistance after the H-transition was reported from JET, ASDEX [2], DIII-D [3], JFT-2M and others. The reason why the coupling resistance decreased after the H-transition has been understood from the steep density gradient [4] or the low density scrape-off-plasma (SOP) as the feature of the H-mode. On the other hand, the increase in coupling resistance during H-mode was firstly observed in JT-60. At first, we report this interesting phenomena about the coupling resistance after the H-mode transition in JT-60. Next, we show the analysis of this phenomena with coupling theory. At last, we show the density dependence of the changing rate of coupling resistance after H-mode transition on JT-60U parameters.

2. EXPERIMENTAL RESULTS IN JT-60

The second harmonic ion cyclotron range of frequency (ICRF) heating is being investigated in JT-60 at the frequency of 120~130 MHz. JT-60 is a circular tokamak which could be operated in an outer single null divertor or a limiter configuration. The major and minor radii of plasma are about 3.1 m and 0.9 m, respectively [5]. JT-60 ICRF launcher consists of a single layer Faraday shield, a 2×2 phased loop antenna array and a metal casing as shown in Fig. 1(a) [6]. The surface of the metal casing is protected by guard limiters made of carbon (both sides) and carbon-carbon composite (top and bottom). We can control the toroidal and poloidal phase differences of the 2×2 loop array. Present experiments have been carried out with $(0,0)$ and $(\pi,0)$ phasing mode as shown in Fig. 1(b). Figure 2 shows the coupling resistance versus line averaged electron density. Solid line shows the theoretical result. The $(\pi,0)$ phasing is characterized as high heating efficiency but small plasma coupling, and the $(0,0)$ phasing is characterized as low heating efficiency but large plasma coupling [7,8].

The H-mode phenomenon was found in the combined ICRF and NBI heating in JT-60 [9]. The interesting phenomena for ICRF coupling property were observed in the H-mode discharges [10]. Figure 3 shows the time evolution of coupling resistance R_c, line integrated electron density $\int n_e d\ell$ at $r/a = 0$ and 0.6, where r and a are the minor radius location and the separatrix location, respectively, H_α emission from a main plasma or a divertor chamber, plasma energy W^* measured by a diamagnetic loop, incident NBI and RF power P_{NB}, P_{IC} for (a) $(\pi,0)$ phasing and (b) $(0,0)$ phasing. The plasma current and toroidal magnetic field were 2.0 MA and 4.5 T in Fig. 3(a), and were 2.7 MA and 4.8 T in Fig. 3(b), respectively. The left vertical broken line and the right one in Fig. 3(a) and Fig. 3(b) indicate the beginning and the end of H-mode, respectively. The electron density increased, the H_α signal decreased and the plasma energy increased during H-mode in both shots. The coupling resistance decreased gradually in $(0,0)$ phasing after the H-transition. These are common features of the H-mode except that the coupling resistance decreases rapidly at the H-transition in other tokamaks. But the coupling resistance increased in $(\pi,0)$ phasing after the H-transition in JT-60.

Figure 4 shows the radial density profiles of the same shots as those of Fig. 3. The solid line and the dashed and dotted line show the L-mode and the H-mode profiles, respectively. The density profiles after the

H-transition were flattened, so that the density gradient inside the separatrix became steep. The density profiles of the main plasma are fitted by

$$n_e(r) = \{n_e(0) - n_e(a)\}\{1 - (r/a)^2\}^m + n_e(a) \qquad (0 \leqq r \leqq a) \tag{1}$$

from the line integrated electron density which were measured by sub-millimeter interferometer at three radial locations (r = -0.6, 0.0 and 0.6 m), where $n_e(a)$ is assumed to be $n_e(0)/10$. The density profile of the SOP which is experimentally quite uncertain at JT-60 is assumed as follows,

$$n_e(r) = n_e(a)\ e^{-(r-a)/\lambda_e} \qquad (a \leqq r \leqq c) \tag{2}$$

where c and λ_e are the location of the protection plate of the first wall and the e-folding length of electron density in SOL. λ_e are assumed to be 0.03 m in Fig. 4. The broken lines in Fig. 4 show the locations of the fast wave cut-off surfaces for various values of toroidal wave number $k_\parallel$ of the fast wave. The cut-off dènsity of the fast wave n_e^c is given by

$$n_e^c \simeq (\varepsilon_0 B/e)(\omega + Z_i dB/m_i)N_z^2 \tag{3}$$

where ε_0, B, Z_i, ω, m_i, and N_z are the dielectric constant in free space, the magnetic field, the ion charge, the angular frequency of the injected RF power, the ion mass and the toroidal refractive index of the fast wave. Ranges of $k_\parallel$ which occupy a large fraction of the $k_\parallel$ spectra of the antenna currents in (0,0) and (π,0) phasing are 0~8 m^{-1} and 12~24 m^{-1}, respectively. In (0,0) phasing, the cut-off surfaces corresponding to the $k_\parallel$-range mentioned above were placed in SOL (Fig. 4(b)), so that a evanescent layer in front of the launcher became thicker after the H-transition. On the other hand, in (π,0) phasing, those were placed inside separatrix (Fig. 4(a)), so that the evanescent layer became thinner after the H-transition. Then, the coupling resistances in (0,0) phasing decreased and those in (π,0) phasing increased after the H-transition. Therefore, the difference of the R_c behaviors in both phasings during the H-mode can be understood by the difference of the $k_\parallel$ spectra of antenna currents.

3. CALCULATION RESULTS FOR JT-60

The coupling resistances of the 2 × 2 loop antennas during H-mode were calculated with the 3-D antenna coupling code, where the density profiles in Fig. 4 are used with slab plasma model [11,12]. To estimate the effect of the change of SOP density on the coupling resistance, two density profiles with and without SOL are assumed in H-mode, while only one density profile with SOL is assumed in L-mode. The toroidal interval of current straps were scanned with the toroidal phase difference of π or zero radian in order to estimate the dependence of coupling resistance on the $k_{\parallel}$ spectrum. Figure 5 shows the changing rate of the coupling resistance before and after the H-transition $\Delta R_c/R_c^{\text{L-mode}}$ ($\Delta R_c = R_c^{\text{H-mode}} - R_c^{\text{L-mode}}$) versus the toroidal interval of current straps d for (a) (π,0) phasing and (b) (0,0) phasing. The solid lines and the broken lines indicate the R_c changing rate from L-mode profile to H-mode one with SOL and to H-mode one without SOL, respectively. The closed circles indicate the experimental data. The experimental data can be explained by the theory, qualitatively. The difference between the solid line and the broken line in Fig. 5 shows the decrement of the coupling resistance due to the decrement of SOP density. $\Delta R_c/R_c^{\text{L-mode}}$ decreases gradually from positive to negative with the toroidal interval of current straps in (π,0) phasing as shown in Fig. 5(a). If the toroidal interval of current straps is the value where the changing rate becomes around zero, the coupling resistances do not change after the H-transition so much. In (0,0) phasing, the changing rate of the coupling resistance is always negative as shown in Fig. 5(b). These results mean that it is possible to control the changing rate of coupling resistance after the H-transition by adjusting the $k_{\parallel}$ spectrum, which is decided by the toroidal interval and the toroidal phase difference between the both antennas.

Figure 6 shows the coupling resistances versus the toroidal interval of current straps for (a) (π,0) phasing and (b) (0,0) phasing. The solid line shows the coupling resistance in the L-mode profile. The broken line and the dashed and dotted line show those in the H-mode profiles with and without SOL, respectively. The closed circle and the open circle indicate the experimental data in L-mode and H-mode, respectively. The two experimental data points are roughly consistent with theory, as shown in Fig. 3(b). If the toroidal interval of current straps is the value where the changing rate becomes around zero, the coupling resistance is twice as large as that of present JT-60 launcher.

Figure 7 shows the $k_{\parallel}$ spectra of the real parts of antenna impedance, i.e. the $k_{\parallel}$ spectra of the radiated power, for (a) $(\pi,0)$ phasing and (b) (0,0) phasing before and after the H-transition with JT-60 launcher parameters. The density profiles in Fig. 4 are used for this calculation. The solid line shows the spectrum in L-mode. The broken line and the dashed and dotted line show spectra in H-mode with and without SOL, respectively. The difference between the solid line and the broken line indicates the effect by the change of density profile inside the separatrix. The $k_{\parallel}$ spectrum below 10 m^{-1} decreases by the increase in the wave impedance gradient due to the increase in the electron density gradient near the separatrix for both phasing. But the $k_{\parallel}$ spectrum more than 10 m^{-1}, which only exists for $(\pi,0)$ phasing, increases by the shift of the cut-off surface to the antennas. The difference between the broken line and the dashed and dotted line indicates the effect of the SOP density on the plasma coupling. The $k_{\parallel}$ spectra below 12 m^{-1} decrease by the decrement in the SOP density, but the $k_{\parallel}$ spectra more than 12 m^{-1} do not change. The most part of the $k_{\parallel}$ spectrum in (0,0) phasing decreases, but the $k_{\parallel}$ spectrum in $(\pi,0)$ phasing shifts to higher $k_{\parallel}$ value so that the coupling resistance increases after H-mode transition.

4. CALCULATION RESULTS FOR JT-60U

JT-60U, which is planed to be made by using JT-60 toroidal coils, is a non-circular tokamak which can be operated in lower single null divertor or limiter configurations. Maximum plasma current is planed to be 6 MA on limiter operation. To investigate the coupling property in JT-60U during H-mode, the coupling resistance of the toroidal 4 loop antenna array as shown in Fig. 8 was calculated in high density regime with JT-60U parameters (R = 3.4 m, a = 1.08 m). A metal casing is not taken into account in the coupling theory. The density profile is assumed to be with SOL in L-mode and without SOL in H-mode, which are the same as assumed in calculation for JT-60. At the same of the assumed that for JT-60. The density profile parameter m in Eq. 1 for L and H-mode were assumed to be those in Fig. 4 (b) (m = 0.5 in L-mode and m = 0.195 in H-mode).

The averaged coupling resistance of 4 loop antennas versus the toroidal interval of current straps for $(0,\pi,0,\pi)$ phasing is shown in Fig. 9, where the values in parenthesis indicate the current phase of toroidal 4 loop antenna array. The solid line and the broken line show the coupling

Figure 7 shows the $k_{\parallel}$ spectra of the real parts of antenna impedance, i.e. the $k_{\parallel}$ spectra of the radiated power, for (a) $(\pi,0)$ phasing and (b) (0,0) phasing before and after the H-transition with JT-60 launcher parameters. The density profiles in Fig. 4 are used for this calculation. The solid line shows the spectrum in L-mode. The broken line and the dashed and dotted line show spectra in H-mode with and without SOL, respectively. The difference between the solid line and the broken line indicates the effect by the change of density profile inside the separatrix. The $k_{\parallel}$ spectrum below 10 m^{-1} decreases by the increase in the wave impedance gradient due to the increase in the electron density gradient near the separatrix for both phasing. But the $k_{\parallel}$ spectrum more than 10 m^{-1}, which only exists for $(\pi,0)$ phasing, increases by the shift of the cut-off surface to the antennas. The difference between the broken line and the dashed and dotted line indicates the effect of the SOP density on the plasma coupling. The $k_{\parallel}$ spectra below 12 m^{-1} decrease by the decrement in the SOP density, but the $k_{\parallel}$ spectra more than 12 m^{-1} do not change. The most part of the $k_{\parallel}$ spectrum in (0,0) phasing decreases, but the $k_{\parallel}$ spectrum in $(\pi,0)$ phasing shifts to higher $k_{\parallel}$ value so that the coupling resistance increases after H-mode transition.

4. CALCULATION RESULTS FOR JT-60U

JT-60U, which is planed to be made by using JT-60 toroidal coils, is a non-circular tokamak which can be operated in lower single null divertor or limiter configurations. Maximum plasma current is planed to be 6 MA on limiter operation. To investigate the coupling property in JT-60U during H-mode, the coupling resistance of the toroidal 4 loop antenna array as shown in Fig. 8 was calculated in high density regime with JT-60U parameters (R = 3.4 m, a = 1.08 m). A metal casing is not taken into account in the coupling theory. The density profile is assumed to be with SOL in L-mode and without SOL in H-mode, which are the same as assumed in calculation for JT-60. At the same of the assumed that for JT-60. The density profile parameter m in Eq. 1 for L and H-mode were assumed to be those in Fig. 4 (b) (m = 0.5 in L-mode and m = 0.195 in H-mode).

The averaged coupling resistance of 4 loop antennas versus the toroidal interval of current straps for $(0,\pi,0,\pi)$ phasing is shown in Fig. 9, where the values in parenthesis indicate the current phase of toroidal 4 loop antenna array. The solid line and the broken line show the coupling

resistances in L-mode profile and H-mode one, respectively. The coupling resistance in L-mode is larger than that in H-mode. The difference between the coupling resistances in L-mode and that in H-mode increase with the toroidal interval of current straps.

The averaged coupling resistance of the 4 loop antennas versus the averaged electron density for the both of (0,0,0,0) and $(0,\pi,0,\pi)$ phasing is shown in Fig. 10. The solid line and the broken line show the coupling resistances in L-mode density profile and H-mode one, respectively. In (0,0,0,0) phasing, the coupling resistance in L-mode is always much higher than that in H-mode. The coupling resistance in H-mode decreases and that in L-mode increases with electron density in $(0,\pi,0,\pi)$ phasing. Therefore, the coupling resistance in L-mode is lower than that in H-mode at low density regime, but higher than that in H-mode at high density regime. This result can be explained by the wave impedance gradient and the location of cut-off surface. In H-mode density profile, the density gradient is so steep that the location of cut-off surface which is almost on the separatrix surface is independent on the averaged electron density. However, the wave impedance gradient which increases with the averaged electron density depresses the plasma coupling. In L-mode, the electron density in SOL increases with averaged electron density, so that the cut-off surface shifts to the antennas. Furthermore, the density gradient, that is wave impedance gradient, is not so steep. Therefore, the coupling resistance increases with averaged electron density.

The averaged coupling resistance versus $n_e(a)/n_e(0)$ for $(0,\pi,0,\pi)$ phasing is shown in Fig. 11. The solid line and the broken line show the coupling resistance in L-mode profile and H-mode one, respectively. The reason why the coupling resistance is not affected by the value of $n_e(a)/n_e(0)$ in H-mode is explained with the density gradient nearby separatrix. Because, the density gradient nearby separatrix is so steep that the density profile without SOL in front of the antennas is not affected by the value of $n_e(a)/n_e(0)$. The coupling resistance in L-mode increases with the value of $n_e(a)/n_e(0)$, because the cut-off surface shifts to the antenna with high density SOL.

Figure 12 shows the toroidal wave number spectra of the averaged real parts of antenna impedance over the four loops for $(0,\pi,0,\pi)$ phasing before and after the H-mode transition. The solid line and the broken line show the $k_{\parallel}$ spectra in L-mode density profile and H-mode one. After H-mode transition, the spectra decrease at all $k_{\parallel}$ value, because of the

increase in wave impedance gradient and the decrease in the SOL density. In this calculation, the simple function, that is Eq.(1), is used for density profile. Therefore, the density gradient just inside the separatrix increases with the averaged density. Furthermore, the assumed density profile in H-mode does not have SOL. The above calculation results indicate the changing rate of coupling resistance after H-mode transition decreases from positive to negative with the averaged electron density. But, if the density profile in H-mode is assumed to have SOL, the coupling resistance may decrease not so much.

5. CONCLUSIONS

The coupling property of the loop antenna array was investigated after H-mode transition for JT-60 and JT-60U. The changing rate of the coupling resistance after H-transition was positive in $(\pi,0)$ phasing, but negative in (0,0) phasing in JT-60 experiment. These phenomena agree qualitatively with the coupling theory taking account of the antenna phasing and the electron density profile. The changing rate of coupling resistance after the H-mode transition depends on the $k_{\parallel}$ spectrum of the radiated power and the density profile near by separatrix. In low density regime, it should be possible to keep the coupling resistance constant after the H-transition by selecting the optimum toroidal interval of current straps and adjusting the toroidal phase difference between them. But, in high density regime such as JT-60U, the decrease in coupling resistance of the toroidal 4 loop antenna array is predicted by the coupling theory in the both of (0,0,0,0) and $(0,\pi,0,\pi,0)$ phasing.

ACKNOWLEDGEMENTS

We would like to thank Drs. M. Tanaka, T. Iijima, M. Yoshikawa, K. Tomabechi, Y. Iso and S. Mori for their continuous encouragement.

increase in wave impedance gradient and the decrease in the SOL density. In this calculation, the simple function, that is Eq.(1), is used for density profile. Therefore, the density gradient just inside the separatrix increases with the averaged density. Furthermore, the assumed density profile in H-mode does not have SOL. The above calculation results indicate the changing rate of coupling resistance after H-mode transition decreases from positive to negative with the averaged electron density. But, if the density profile in H-mode is assumed to have SOL, the coupling resistance may decrease not so much.

5. CONCLUSIONS

The coupling property of the loop antenna array was investigated after H-mode transition for JT-60 and JT-60U. The changing rate of the coupling resistance after H-transition was positive in $(\pi,0)$ phasing, but negative in (0,0) phasing in JT-60 experiment. These phenomena agree qualitatively with the coupling theory taking account of the antenna phasing and the electron density profile. The changing rate of coupling resistance after the H-mode transition depends on the $k_{\parallel}$ spectrum of the radiated power and the density profile near by separatrix. In low density regime, it should be possible to keep the coupling resistance constant after the H-transition by selecting the optimum toroidal interval of current straps and adjusting the toroidal phase difference between them. But, in high density regime such as JT-60U, the decrease in coupling resistance of the toroidal 4 loop antenna array is predicted by the coupling theory in the both of (0,0,0,0) and $(0,\pi,0,\pi,0)$ phasing.

ACKNOWLEDGEMENTS

We would like to thank Drs. M. Tanaka, T. Iijima, M. Yoshikawa, K. Tomabechi, Y. Iso and S. Mori for their continuous encouragement.

increase in wave impedance gradient and the decrease in the SOL density. In this calculation, the simple function, that is Eq.(1), is used for density profile. Therefore, the density gradient just inside the separatrix increases with the averaged density. Furthermore, the assumed density profile in H-mode does not have SOL. The above calculation results indicate the changing rate of coupling resistance after H-mode transition decreases from positive to negative with the averaged electron density. But, if the density profile in H-mode is assumed to have SOL, the coupling resistance may decrease not so much.

5. CONCLUSIONS

The coupling property of the loop antenna array was investigated after H-mode transition for JT-60 and JT-60U. The changing rate of the coupling resistance after H-transition was positive in $(\pi,0)$ phasing, but negative in (0,0) phasing in JT-60 experiment. These phenomena agree qualitatively with the coupling theory taking account of the antenna phasing and the electron density profile. The changing rate of coupling resistance after the H-mode transition depends on the $k_{\parallel}$ spectrum of the radiated power and the density profile near by separatrix. In low density regime, it should be possible to keep the coupling resistance constant after the H-transition by selecting the optimum toroidal interval of current straps and adjusting the toroidal phase difference between them. But, in high density regime such as JT-60U, the decrease in coupling resistance of the toroidal 4 loop antenna array is predicted by the coupling theory in the both of (0,0,0,0) and $(0,\pi,0,\pi,0)$ phasing.

ACKNOWLEDGEMENTS

We would like to thank Drs. M. Tanaka, T. Iijima, M. Yoshikawa, K. Tomabechi, Y. Iso and S. Mori for their continuous encouragement.

REFERENCES

[1] LACKNER, K., DITE, U., FUSSMANN, G., GRAVE, T., JANESCHITZ, G., et al.,; in Plasma Physics and Controlled Nuclear Fusion Research (Proc. 10th Int. Conf. London, 1984), Vol. 1 IAEA, Vienna (1985) 319.

[2] STEINMETZ, K., ICRF Heating in Fusion Plasmas, on Applications of Radio Frequency Power to Plasmas, (Proc. 7th Top. conf. Kissimmee, Florida, 1987), Conf. Proc. No. 159, American institute of physics, New York (1987) A2.

[3] MAYBERRY, M.J., BAITY, F.W., HOFFMAN, D., LUXON, J.L., OWENS, T.L. et al., Coupling of an ICRF Compact Loop Antenna to H-Mode Plasma in DIII-D, on Applications of Radio Frequency Power to Plasmas, (Proc. 7th Top. conf. Kissimmee, Florida, 1987), Conf. Proc. No. 159, American institute of physics, New York (1987) 278.

[4] MAU, T. K., CHIU, S. C., and BAKER, D. R., IEEE Trans. Plasma Sci., vol. PS-15, NO. 3, (1987) 273.

[5] YOSHIKAWA, M., Nucl. Fusion 25 (1985) 1081.

[6] NAGASHIMA, T., UEHARA, K., KIMURA, H., IMAI, T., FUJII, T., et al., Fusion Engineering and Design 5 (1987) 101.

[7] SAIGUSA, M., KOBAYASHI, N., KIMURA, H., FUJII, T., HAMAMATSU, K., et. al., Coupling Property of ICRF 2 2 Loop Antenna in JT-60, on Applications of Radio Frequency Power to Plasmas, (Proc. 7th Top. conf. Kissimmee, Florida, 1987), Conf. Proc. No. 159, American institute of physics, New York (1987) A25.

[8] KIMURA, H., and JT-60 Team, in Controlled Fusion and Plasma Physics (Proc. 14th Europ. Conf. Madrid, 1987), Vol. 11D, Part III, European Physical Society (1987) 857.

[9] JT-60 Team, Recent Results from JT-60, Japan Atomic Energy Research Institute Report JAERI-M 87-205 (1987).

[10] SAIGUSA, M., KIMURA, H., FUJII, T., KOBAYASHI, N., MORIYAMA, S., et al., submitted to Nucl. Fusion.

[11] KIMURA, H., FUJII, T., IKEDA, Y., SAIGUSA, M., IMAI, T., et al., on Heating in toroidal plasmas (Proc. 4th Int. Symp. Rome, 1984), Vol. II, ECE, Brussels (1984) 1128.

[12] IKEDA, Y., KIMURA, H., FUJII, T., SAIGUSA, M., IMAI, T., et al., Coupling Calculations of the ICRF loop Antenna for JT-60, Japan Atomic Energy Research Institute Report JAERI-M 84-191 (1984).

(a) JT-60 ICRF
2 x 2 PHASED LOOP ANTENNA

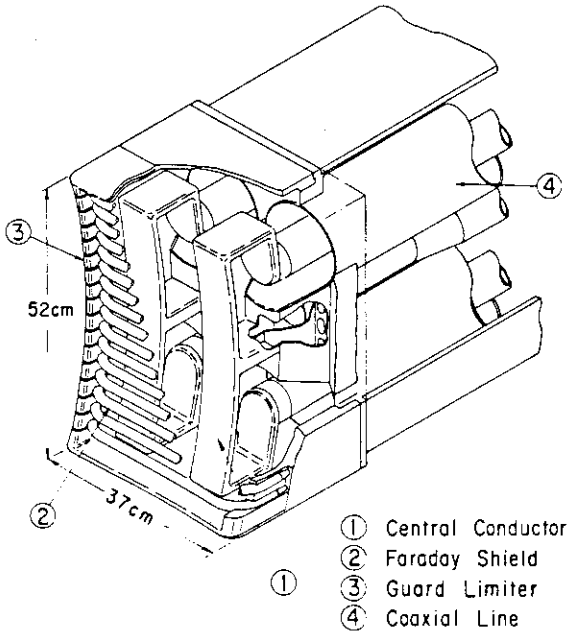

(b)

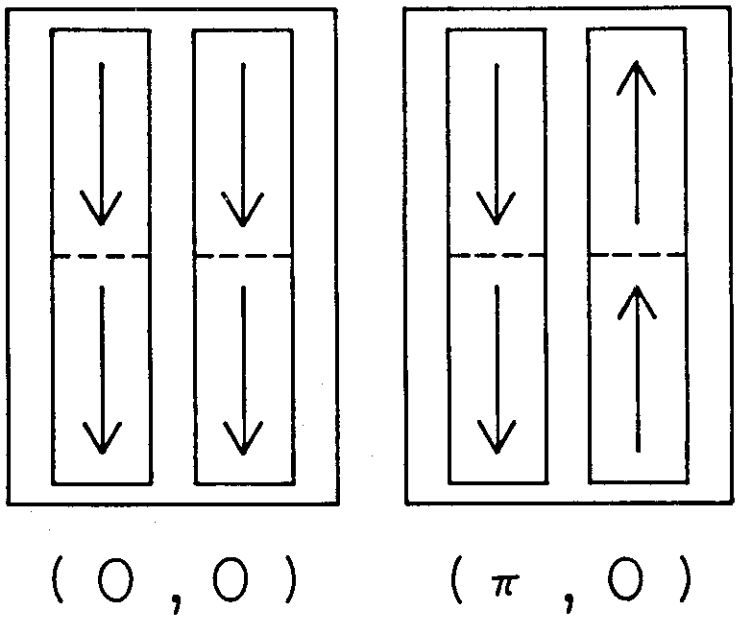

Fig. 1 (a) Structure of the JT-60 ICRF phased loop antenna array.
(b) Antenna phasing modes.

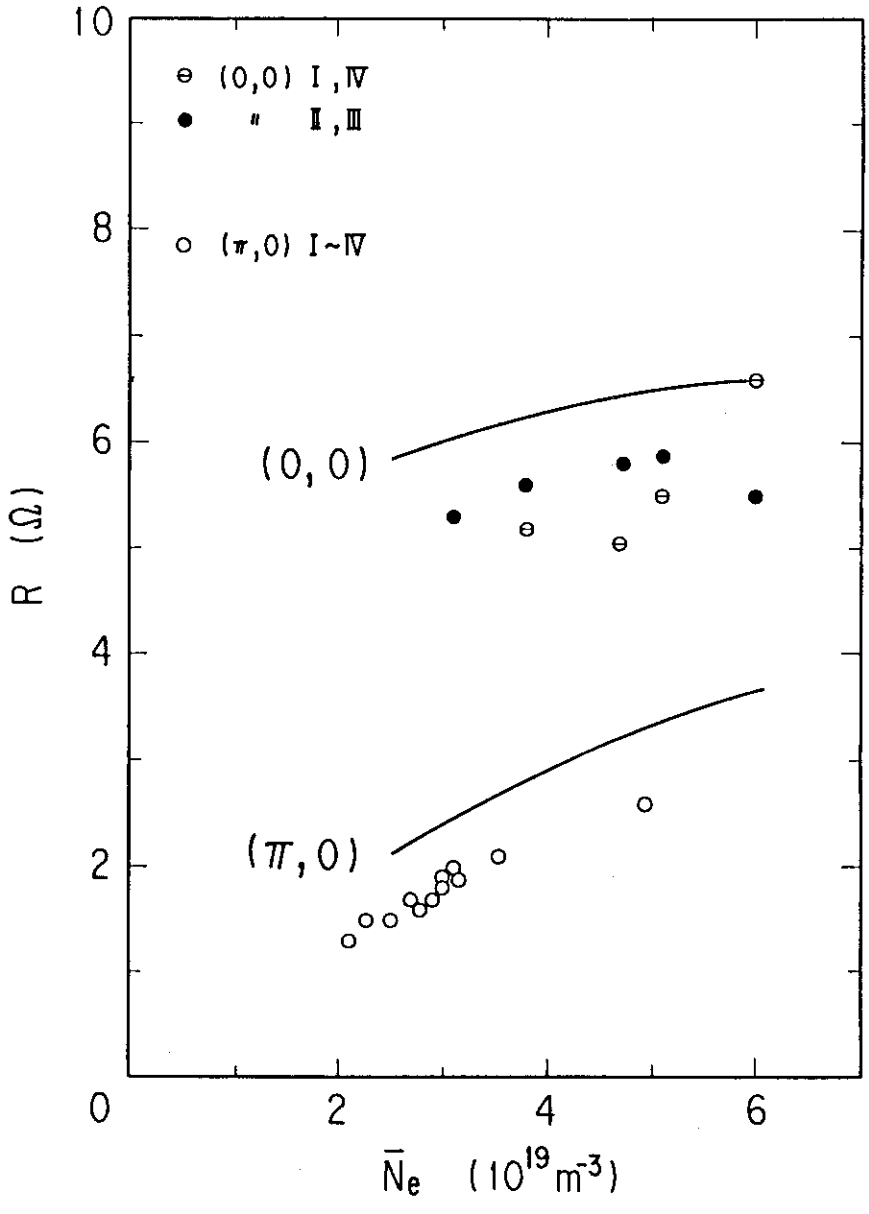

Fig. 2 The coupling resistance versus line averaged electron density. The solid lines show the theory of each phasing.

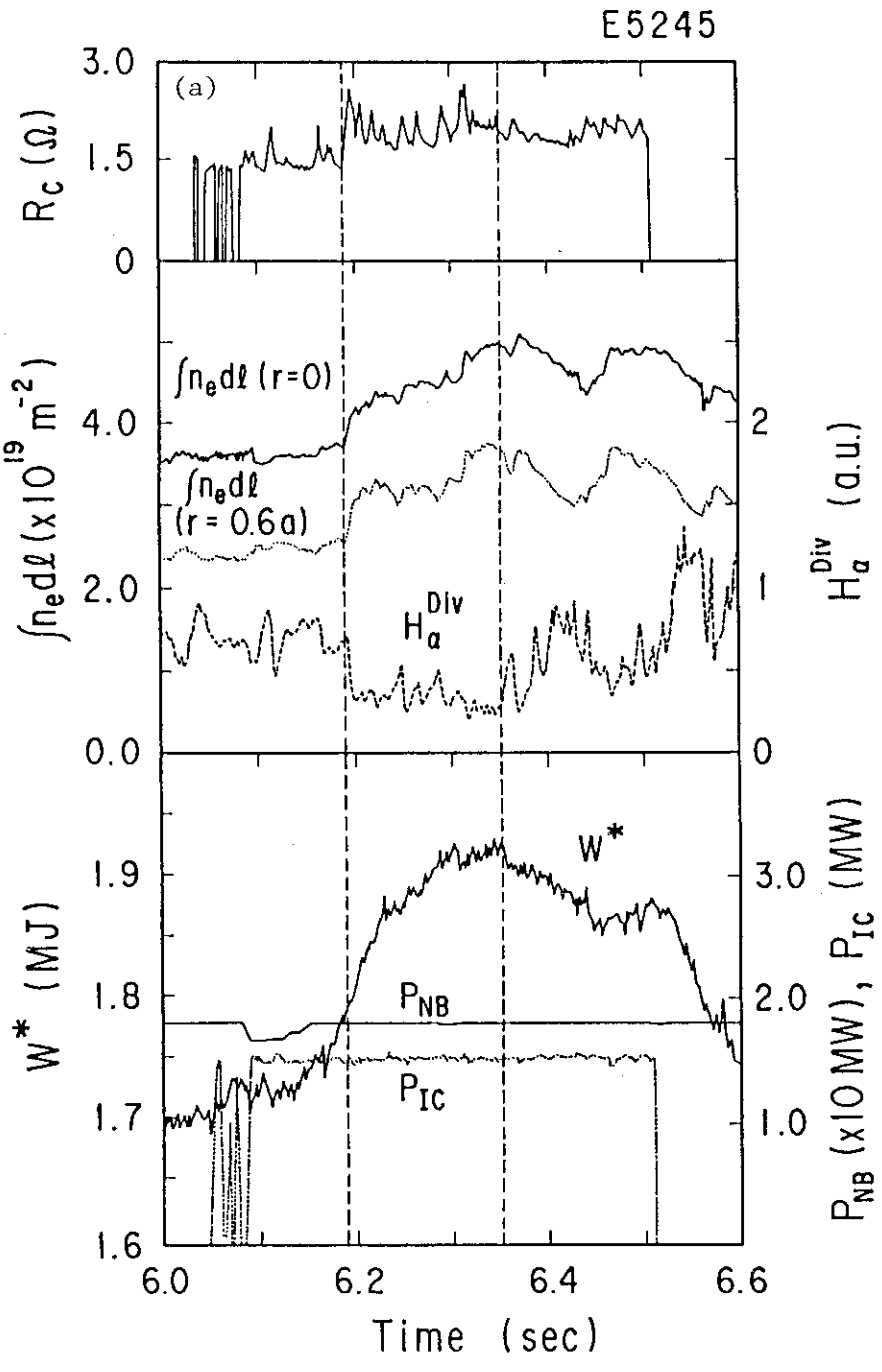

Fig. 3 Time evolution of coupling resistance R_c, line integrated electron density $\int n_e d\ell$ at r/a = 0, 0.6, H_α radiation from the main plasma or the divertor chamber, plasma energy W^*, NBI and RF power P_{NBI}, P_{RF} during H-mode discharges. The left and right broken lines indicate the onset and the end of H-mode, respectively.
(a) $(\pi,0)$ phasing. (b) (0,0) phasing.

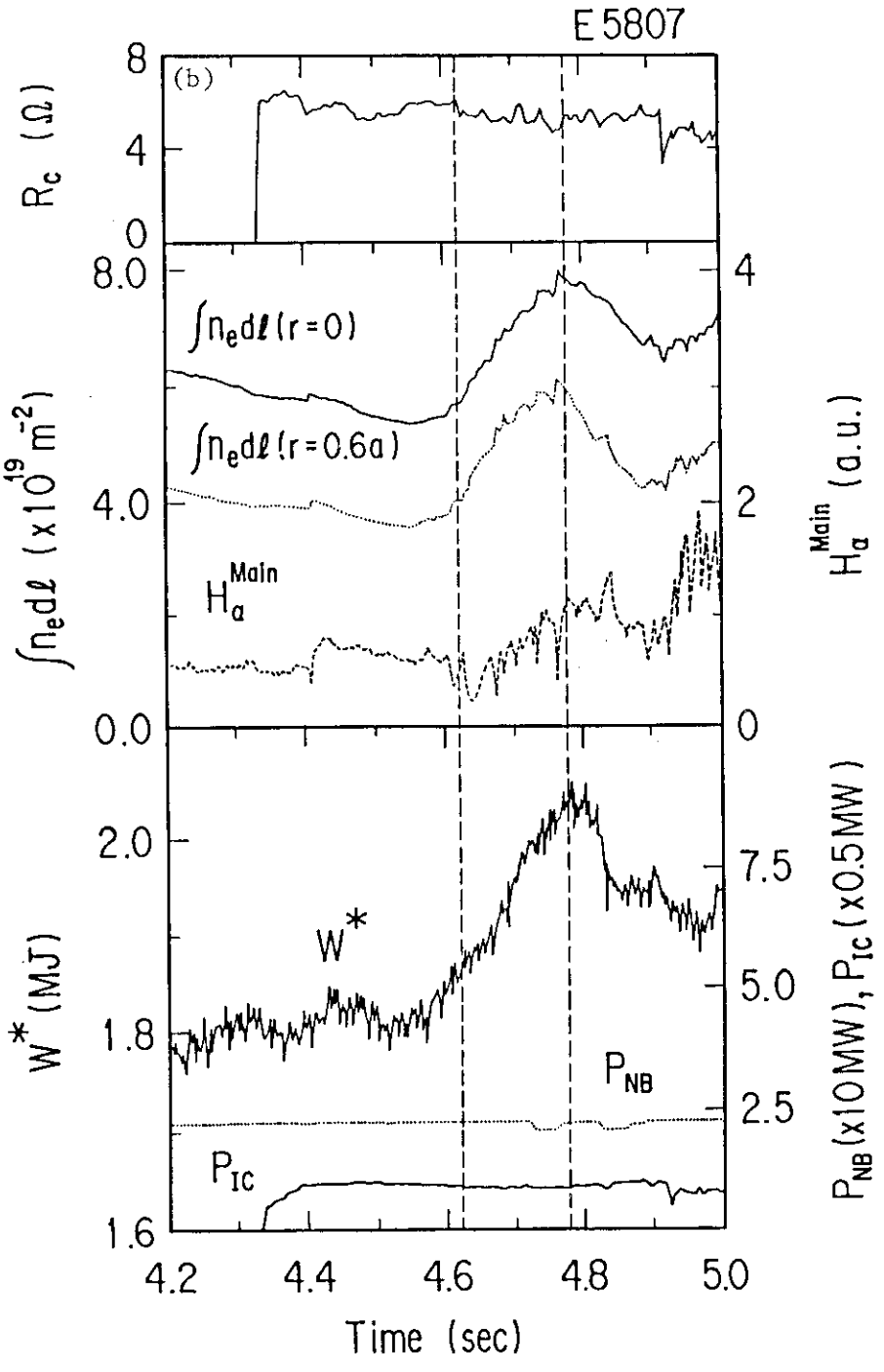

Fig. 3 (Continued)

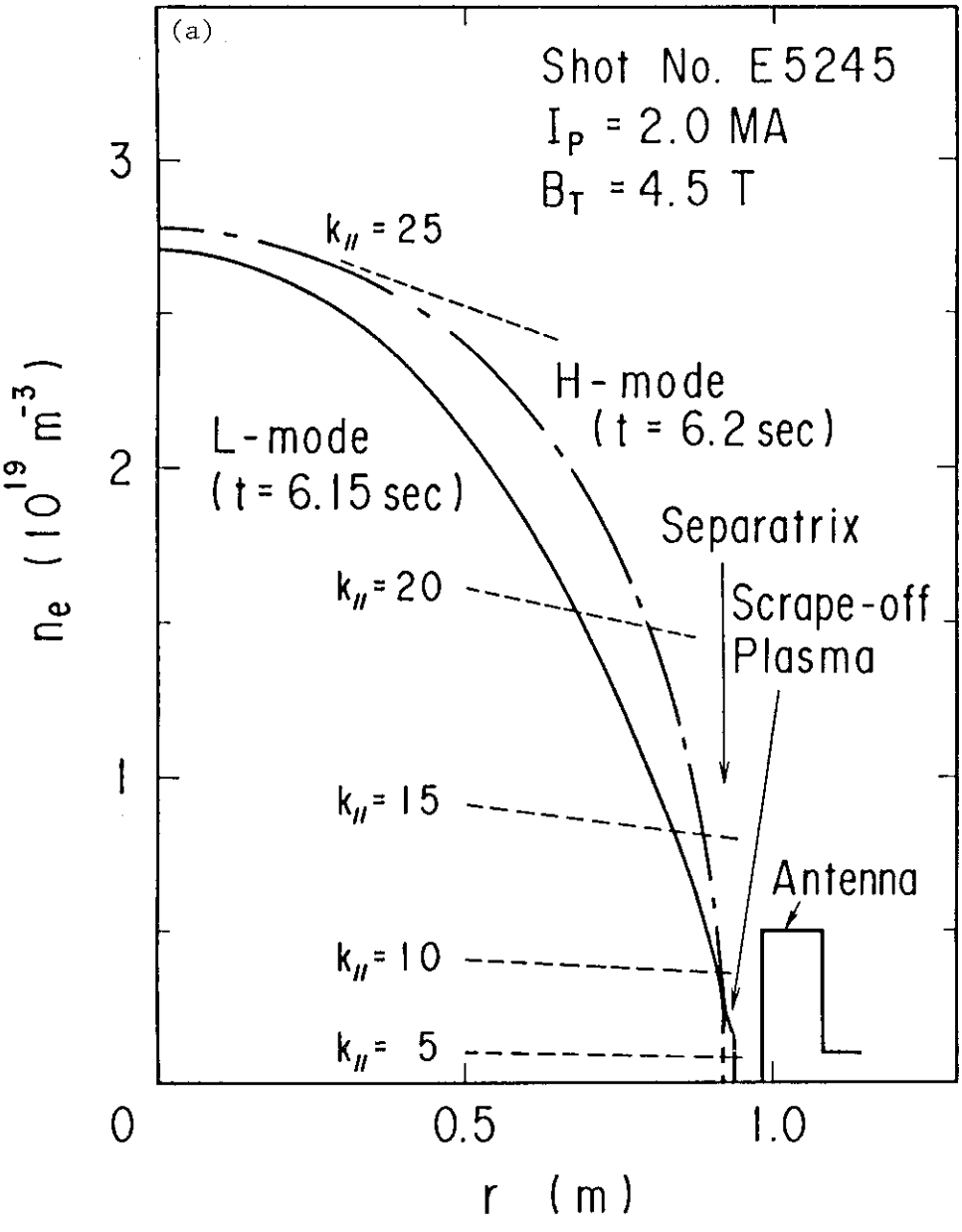

Fig. 4 Electron density profiles before and after the H-mode transition. The solid line and the dashed and dotted line show the L and H-mode profiles, respectively. The broken lines show the cut-off density for various $k_{\parallel}$ values of the fast wave. (a) (π,0) phasing. (b) (0,0) phasing.

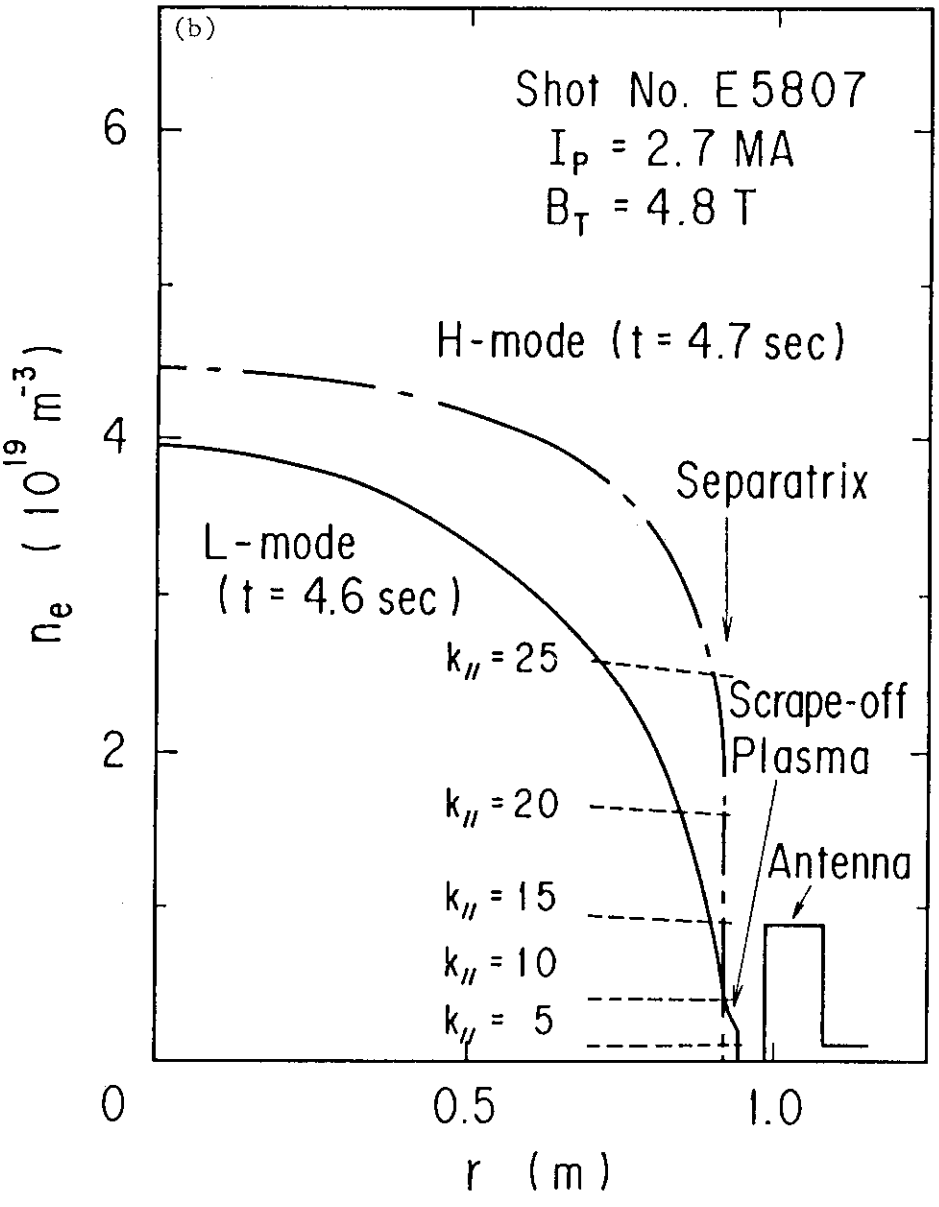

Fig. 4 (Continued)

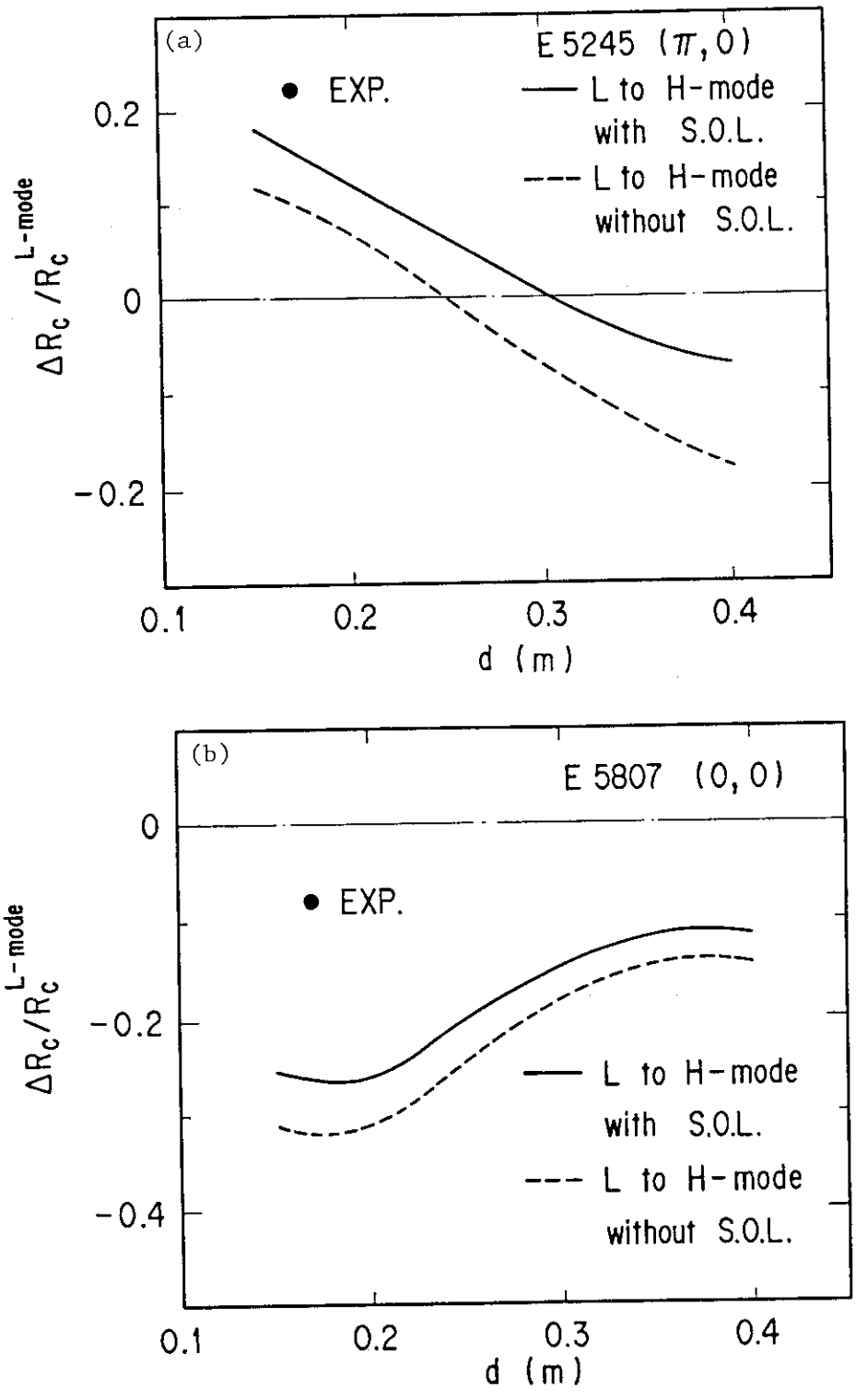

Fig. 5 Changing rate of the coupling resistance $\Delta R_c / R_c^{L\text{-mode}}$ ($\Delta R_c = R_c^{H\text{-mode}} - R_c^{L\text{-mode}}$) versus the toroidal interval of current straps before and after the H-mode transition. The closed circle indicate the experimental data. The solid line indicates $R_c / R_c^{L\text{-mode}}$ from the L-mode profile with SOL to the H-mode one with SOL, and the broken line indicates $\Delta R_c / R_c^{L\text{-mode}}$ from the L-mode profile with SOL to the H-mode one without SOL.
(a) (π,0) phasing. (b) (0,0) phasing.

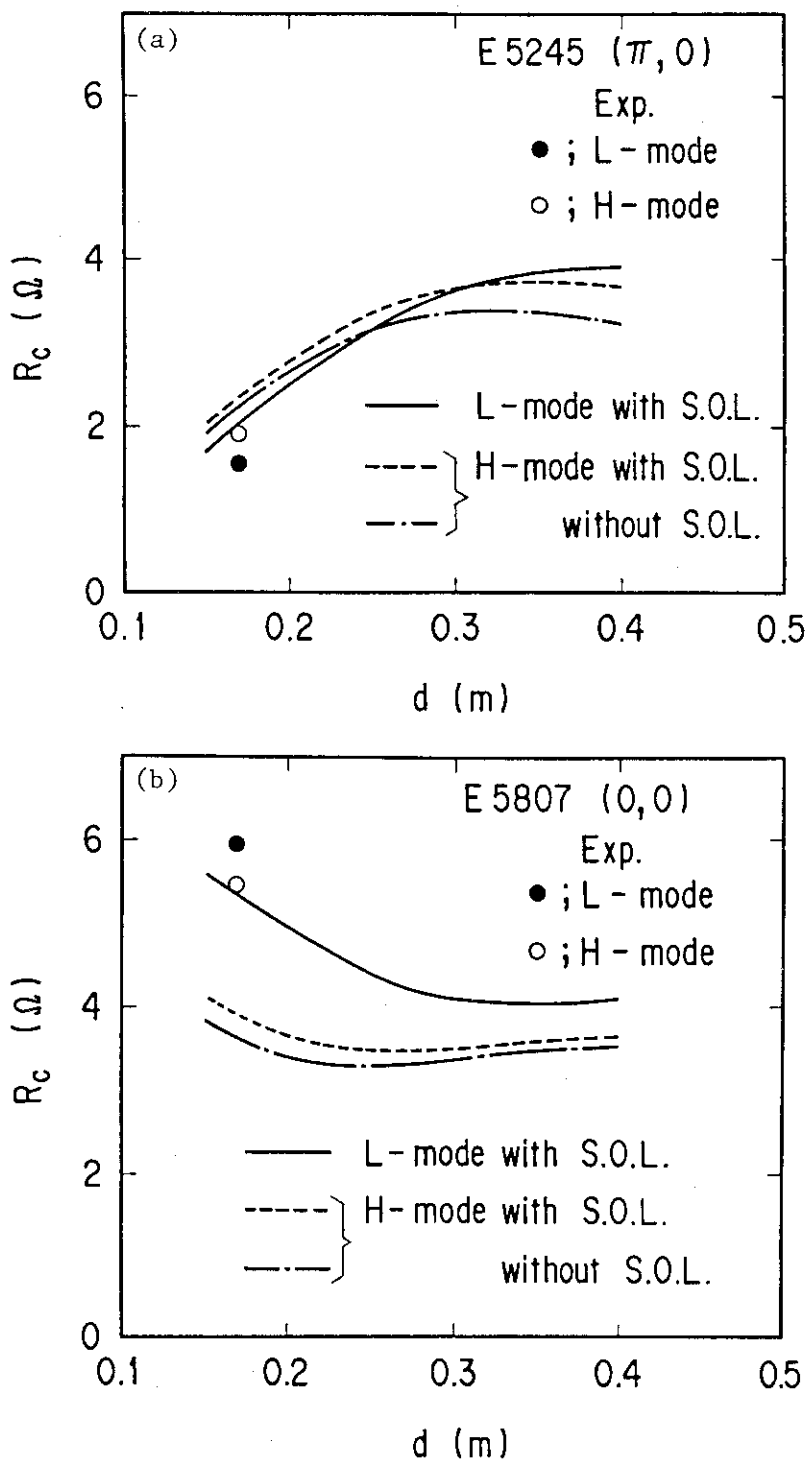

Fig. 6 Coupling resistances versus the toroidal interval of current straps for (a) (π,0) phasing and (b) (0,0) phasing before and after the H-mode transition. The closed and the open circles show the experimental data in L and H-mode, respectively. The solid line, the broken line and the dashed-and-dotted line indicate the results in the L-mode density profile with SOL, in the H-mode profiles with and without SOL, respectively.

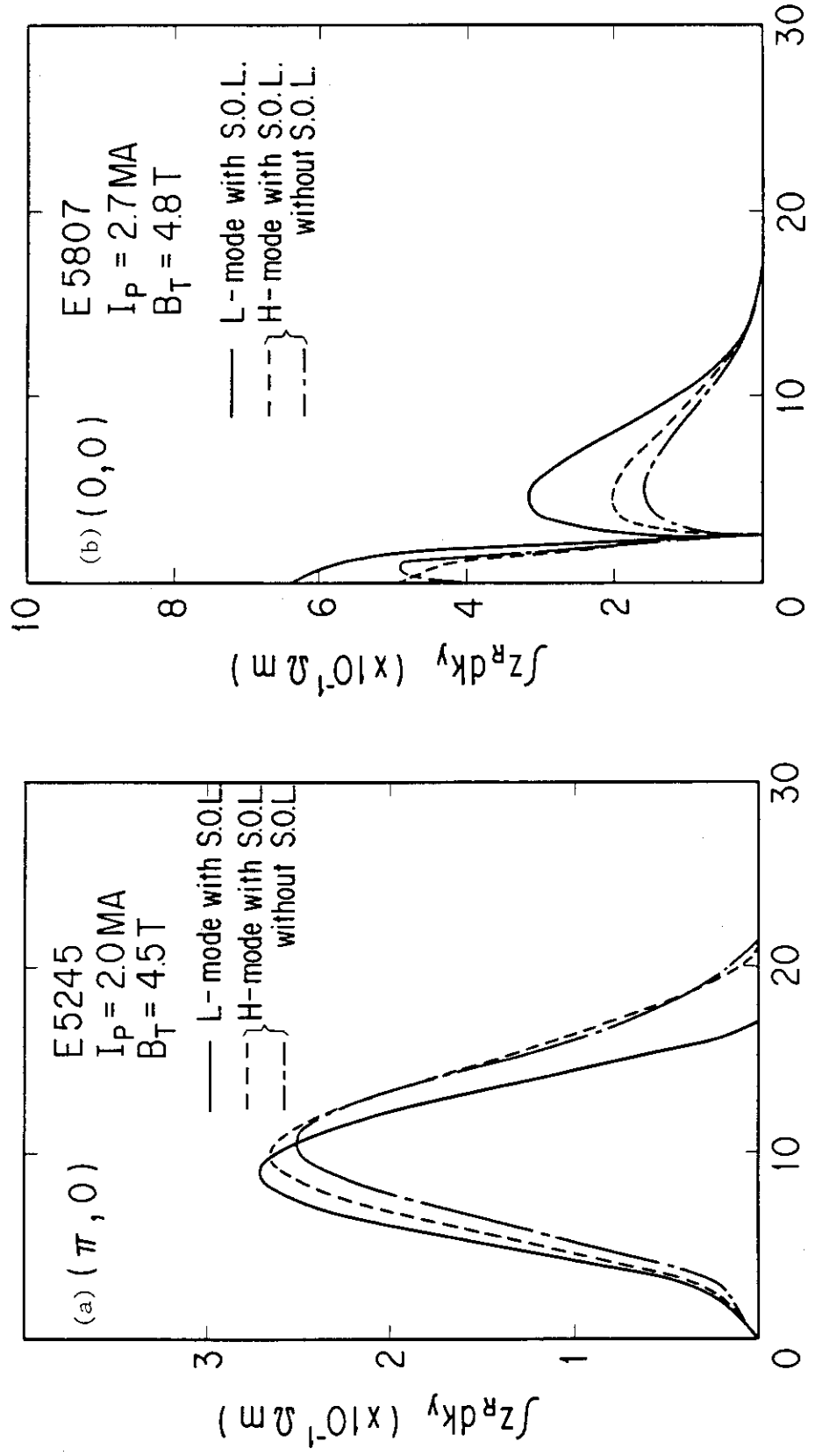

Fig. 7 Toroidal wave number spectra of the real parts of antenna impedance before and after the H-mode transition. The solid line shows the $k_{\parallel}$ spectrum in L-mode density profile. The broken line and the dashed and dotted line show the $k_{\parallel}$ spectra in the H-mode profiles with and without SOL, respectively. (a) (π,0) phasing. (b) (0,0) phasing.

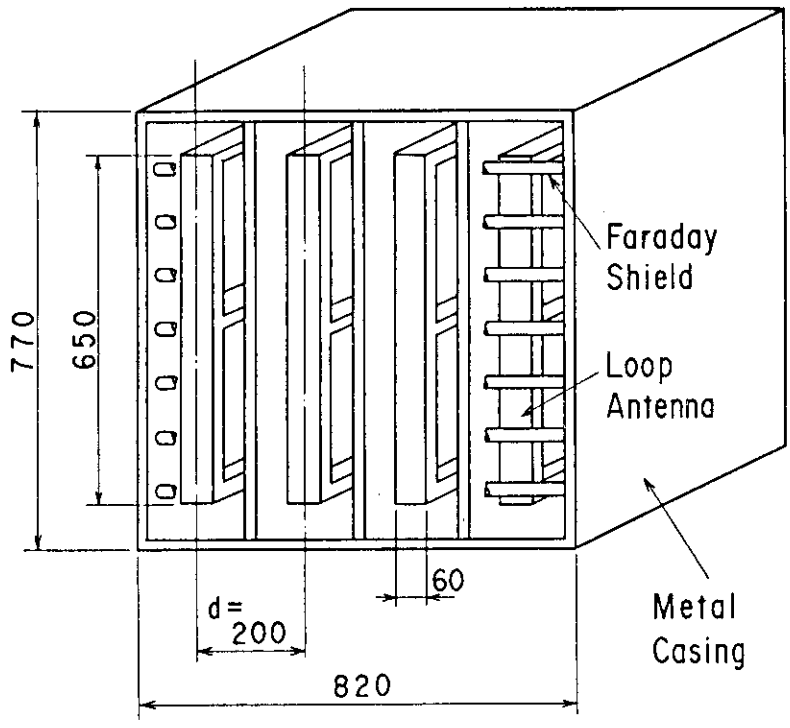

(a) JT-60U 4 Loop Antenna Array

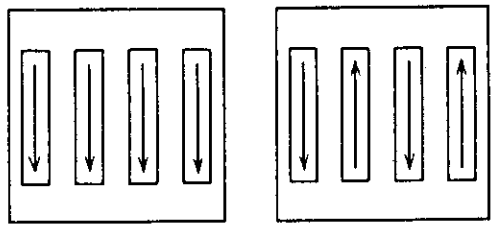

(b) Phasing Mode

Fig. 8 Test designed model of the JT-60U ICRF 4 loop antenna array and antenna phasing modes.

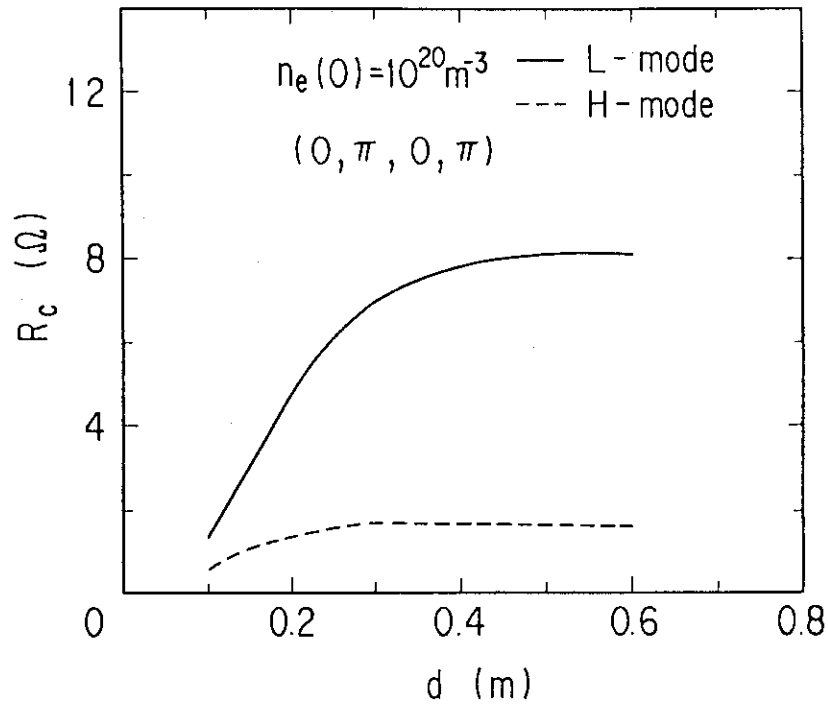

Fig. 9 Averaged coupling resistance of 4 loop antennas versus the toroidal interval of current straps for $(0,\pi,0,\pi)$ phasing. The solid line and the broken line show the coupling resistances in L-mode profile and H-mode one, respectively.

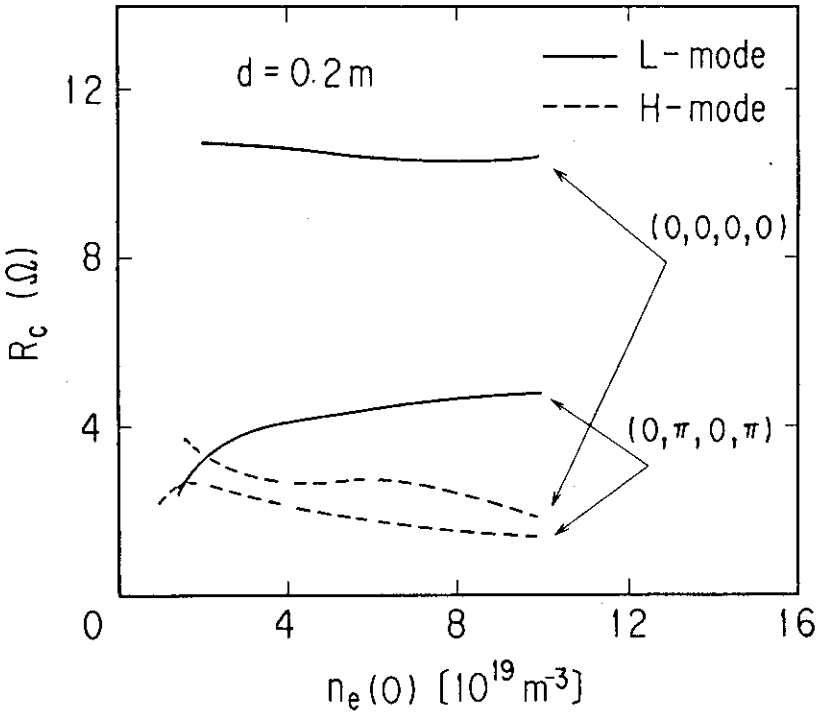

Fig. 10 Averaged coupling resistance of 4 loop antennas versus averaged electron density for both of $(0,0,0,0)$ and $(0,\pi,0,\pi)$ phasing. The solid line and the broken line show the coupling resistance in L-mode density profile and H-mode one, respectively.

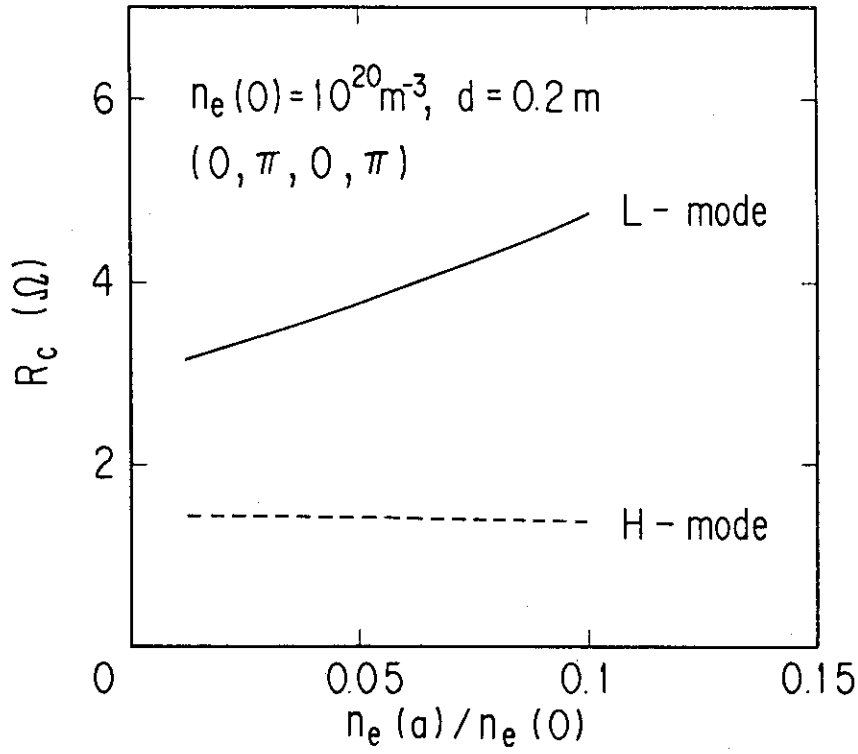

Fig. 11 Averaged coupling resistance of 4 loop antennas versus $n_e(a)/n_e(0)$ for $(0,\pi,0,\pi)$ phasing. The solid line and the broken line show the coupling resistance in L-mode profile and H-mode one, respectively.

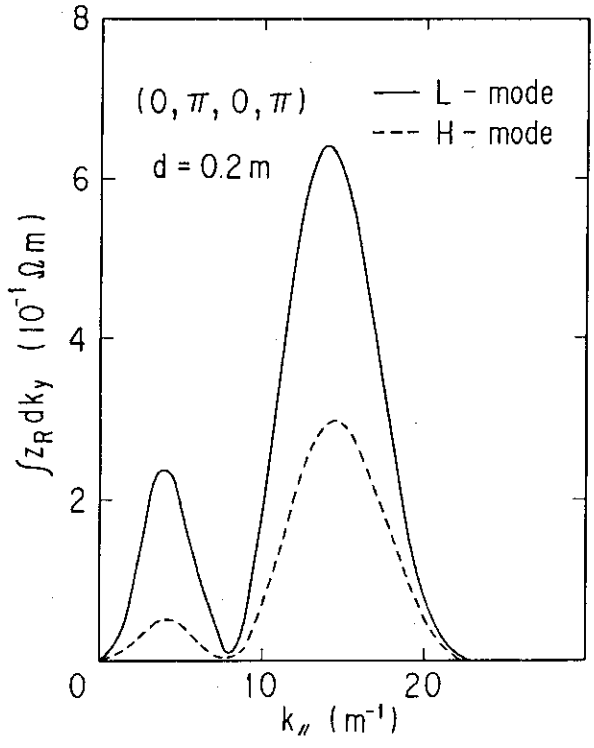

Fig. 12 Toroidal wave number spectra of averaged real parts of antenna impedances for $(0,\pi,0,\pi)$ phasing before and after the H-mode transition. The solid line and the broken line show the $k_{\parallel}$ spectra in L-mode density profile and H-mode one.